Intra-individual methylomics detects the impact of early-life adversity

Shan Jiang*, Noriko Kamei*, Jessica L. Bolton, Xinyi Ma, Hal S. Stern, Tallie Z. Baram†, Ali Mortazavi†

† Corresponding author, email: tallie@uci.edu; ali.mortazavi@uci.edu

* Co-first authors, S. J. and N. K.

Running title: Intra-individual methylome signatures of divergent early-life experiences

Keywords: methylomics, rat, intra-individual, early-life experience

Abstract

Genetic and environmental factors interact during sensitive periods early in life to influence mental health and disease. These influences involve modulating the function of neurons and neuronal networks via epigenetic processes such as DNA methylation. However, it is not known if DNA methylation changes outside the brain provide an 'epigenetic signature' of early-life experiences in an individual child that may serve as a marker for vulnerability or resilience to mental illness. Here, to obviate the massive variance among individuals, we employed a novel intra-individual approach by testing DNA methylation from buccal cells of individual rats before and immediately after exposure to one week of typical or adverse life experience. We show that whereas inter-individual changes in DNA methylation reflect the effect of age, DNA methylation changes within paired DNA samples from the same individual reflect the impact of diverse neonatal experiences on the individual. The methylome signature of early-life experience is enriched in genes encoding transcription factors and key molecular cellular pathways. Specifically, genes involved in cell morphogenesis and differentiation were more methylated in pups exposed to the adverse environment whereas pathways of response to injury and stress were less methylated. Thus, intra-individual methylome signatures indicate large-scale transcription-driven alterations of cellular fate, growth and function. Our observations in rats--that distinct early-life experiences generate specific individual methylome signatures in accessible peripheral cells--should be readily testable in humans.

Introduction

Experience, particularly during sensitive periods early in life, leaves indelible marks on an individual's ability to cope with life's challenges, influencing resilience or vulnerability to emotional disorders (Bale et al. 2010; Klengel and Binder 2015; Nestler et al. 2015; Chen and Baram 2016; Nelson et al. 2007). There is evidence that the mechanisms by which early-life experiences influence the function of neurons and neuronal networks involve modifying the repertoire and levels of gene expression via epigenetic processes (Bale et al. 2010; Klengel and Binder 2015; Nestler et al. 2015; Szyf 2015; Bedrosian et al. 2018; Chen and Baram 2016; Singh-Taylor et al. 2017; Bale 2015; Bohacek and Mansuy 2015; Dias and Ressler 2013). Among epigenetic processes, changes in DNA methylation of individual genes and at the genomic scale have been reported, and these generally correlate with gene expression (Klengel and Binder 2015; Szyf 2015; Peter et al. 2016; Weaver et al. 2004; Nemoda et al. 2015). However, it is not known if DNA methylation changes might provide a useful 'epigenetic signature' of early-life experiences in an individual child. Such a readily-accessible measure might serve as a biomarker for vulnerability or resilience to mental illness. Obviously, it is not possible to repeatedly sample DNA from brain cells in humans in order to assess DNA methylation changes for predicting and preventing disease. Therefore, current approaches employ peripheral cells including white blood cells (WBC) or buccal swabs (mixed epithelial/WBC), which are available repeatedly and noninvasively. Here we tested the feasibility of using peripheral DNA samples to assess the impact of diverse neonatal experiences on an individual by directly comparing two samples collected at different time points from the same individual rat in groups exposed to distinct early-life experiences with defined onset and duration. We have previously established that these diverse experiences provoke specific phenotypic outcomes later in life (Chen and Baram 2016; Ivy et al. 2010; Bolton et al. 2018). Specifically, we imposed 'simulated poverty' by raising pups for a week (from postnatal day P2 to P10) in cages with limited bedding and nesting materials (LBN). This manipulation disrupts the care provided by the rat dam to her pups and results in profound yet transient stress in the pups, devoid of major weight-loss or physical changes. This transient experience provokes significant and life-long deficits in memory and generates increases in emotional measures of anhedonia and depression (Ivy et al. 2010; Bolton et al. 2018; Lister et al. 2013).

Here we tested if adversity during a defined sensitive developmental period in rats leads to a detectable epigenomic signature in DNA from buccal-swab cells. We obtained intra-individual epigenomic signatures of early-life adversity using reduced representation bisulfite sequencing (RRBS) (Meissner et al. 2005) to identify changes in DNA methylation profiles. Comparisons were

made both between two samples from an individual rat (P2 vs P10) and between samples from rats subjected to the two neonatal experiences. We found that assessing the overall methylation profile of samples enabled detection of age and development effects (Lister et al. 2013; Reizel et al. 2018), distinguishing P2 samples from those obtained on P10, but did not separate the two groups of pups based on their experience. In contrast, the changes in DNA methylation in two samples obtained from the same rat enabled clear differentiation of the control vs the adverse experience, likely by obviating large inter-individual variance. Thus, our findings establish the feasibility of identifying markers of adverse experiences that portend risk or resilience to mental illness, with major potential translational impact.

Results

Methylation changes reflect postnatal age rather than maternal experiences

We obtained a mix of epithelial & white blood cell DNA from rat pups, on P2 and on P10 from the same pup using buccal swabs (Methods). We obtained buccal swabs rather than peripheral white blood cells for three reasons. First, the swab, lasting seconds, is much less stressful than a painful needle prick to obtain peripheral blood, and this stress might influence methylation in itself. Second, this approach provides a more direct comparison with human studies where ethical reasons preclude needle pain whereas buccal swabs are routinely implemented (Said et al. 2014; Lowe et al. 2013). Finally, several studies found that DNA methylation profiles in buccal swab cells are more similar to patterns from several brain regions than methylation profiles in white blood cells (Lowe et al. 2013; Braun et al. 2017; Smith et al. 2015; Davies et al. 2012). Following the initial sample collected on P2, rats were exposed to either simulated poverty or to a typical environment for one week, followed by a second sample on P10. We examined for intra-individual epigenomic signatures of early-life adversity and compared both P10 samples from groups with two divergent neonatal experiences as well as the changes in methylation levels between matched samples from the same individual rat (P2 vs P10; Fig.1A).

DNA methylation status was assessed using RRBS, with libraries sequenced to an average of 20 Million mapped reads, and we reliably detected an average of 482 thousand CpGs in both time points of the same individual (Fig.S1; Methods). We performed differential methylation analysis between P2 and P10 for each individual and identified 3417 significantly differential methylation regions (DMRs) after coalescing CpGs within 100 basepairs that were shared in at least two individuals from each experience group (Figure 1B). These were further analyzed. Specifically, we analyzed the DNA methylation levels of these DMRs in P2 and in P10 for both

the control and adversity-experiencing (LBN) groups across individuals using k-means clustering and observed substantial changes in DNA methylation level during the one-week interval in both control and LBN (Figure 2A). The DNA methylation levels within a given individual clearly distinguished rats at different ages (Figure 2A). We further performed principal component analysis (PCA) on the percentage of DNA methylation of these DMRs and found that individual samples were clearly separated by age using the first three principal components (up to 62.1% variances explained), indicating the large change in DNA methylation associated with age (Figure 2B). Note that this result held when cohort effects were considered (Figure S2B,F; S3A-C). These data demonstrate that development and age modify the buccal swab methylome (Reizel et al. 2018; Smith et al. 2015; Eipel et al. 2016; Horvath and Raj 2018) in conjunction with experience. We then examined the DMRs with the top weights in PC2, which explained 20.7% of the variance and was the dominant component distinguishing individuals of different ages (Figure 2B). We found that DMRs with reduced methylation level in P10 were associated with genes involved in cellular response to hormones, negative regulation of growth and regulation of kinase activity whereas DMRs with increased methylation level in P10 were enriched with genes in pattern specification processes such as nervous system and mesodermal development (Figure S4). Notably, the PCA analyses of the P2 and P10 methylome profiles did not separate the control group from the adversity-experiencing group (Figure 2C). Thus, whereas the level of DNA methylation in buccal swabs may denote an epigenetic signature of age, it provides little information about antecedent life experiences.

Intra-individual changes in methylation can distinguish early-life experience

To probe the impact of the early-life adversity experienced by an individual on DNA methylation patterns of the same individual, we explored intra-individual fold changes in methylation (referred to as “delta methylation”) rather than the absolute value of methylation levels for each pup by taking advantage of the two samples collected immediately before and after a week of imposed adversity. We clustered and aligned these delta methylation profiles (differential methylation between P2 and P10 defined as $\log_2$(P10/P2)) in both early-life experiences (Figure 3A). We then examined the intra-individual methylation changes in detail and found that the patterns of changes in methylation within an individual were distinct depending on group assignment (Figure 3A). We performed a PCA analysis on the individual delta methylation samples and the resulting principal components revealed that delta methylation within an individual clearly distinguished the control and LBN groups (Figure 3B). Specifically, the first three principal components accounted for 65.0% of the variance and the third principal component (PC3)

(4.9% of the variances) distinguished most LBNs from controls. Importantly, the adverse and control experiences differentially reduced or increased levels of methylation in an experience-specific manner. These results indicate that intra-individual changes in methylation-level profiles before and after a defined experience provide a novel epigenetic signature that identifies the nature of the experience.

Differential methylation regions are at the vicinity of multiple transcription factors

The paragraph above demonstrates that levels of DNA methylation in mixed epithelial / white blood cell samples from buccal swab can separate pups by age, whereas the nature of methylation changes in the same individual (delta methylation) distinguishes different early-life experiences. We examined the relative contribution of individual DMRs to the overall difference in PC3, and, guided by the slope of the weight distribution selected a cutoff threshold at +/- $2x10^{-2}$ (Figure 4A) to identify the 346 largest positive weights that account 254 DMRs, which are associated with 246 genes (Figure 4A, Supplemental Figure S6, Supplemental Table 1). The methylation regions with maximal positive weights are thus major contributors to the differential methylation profiles of early-life adversity (LBN) compared to typical development, and genes that have generally increased DNA methylation after the LBN experience typically denote reduced expression. Gene Ontology (GO) analysis of these “positive weight” genes identified enrichment in terms associated with cell and organ development and cell-morphogenesis (Figure 4B). Inspection of individual “positive weight” genes contributing to the adversity-provoked methylome signature uncovered a strong enrichment of genes involved in growth and response to growth factors (26/246 annotated genes; 10.6%), pathways of injury, inflammation, and death (25/246 annotated genes; 10.2%), as well as transcription factors (15/246; 6.1%).

A strongly regulated program of gene expression was also suggested when the same approach was applied to the top 311 negative weights (241 DMRs) associated with 225 genes that contributed most to the methylome signature associated with a typical developmental epoch. First, GO analysis indicated enrichment in genes involved in cell morphogenesis and differentiation. Notably, inspection of the individual “negative weight” genes uncovered likely mechanisms for a regulated gene expression program: 17.8% of the genes in this group (40/225: 17.8%) were transcription factors. Indeed, transcription factors accounted for 30% (7/23) of the top-contributing genes (genes associated with DMRs having weights more significant than $-5x10^{-2}$ in Figure 4A) to the typical methylation phenotype. Further, 53 of the 225 negative weight genes

(23.6%) were involved in cell morphogenesis, cytoskeleton stability and growth, and cell-cell communication.

Discussion

In summary, we find here that comparing cohort-wide DNA samples obtained at different developmental ages reveals the signature of age and development on the peripheral methylome, as widely reported. However, these inter-individual analyses do not distinguish the divergent impacts of diverse experiences that take place during the intervening developmental epoch. By contrast, here we demonstrate that paired samples from the same individual before and after an adverse or typical developmental experience enable clear distinction of each of these experiences: we identify epigenetic 'scars' and 'kisses' on developmentally important genes that, at least in the rodent model, precede and predict later-life emotional functions.

Although it is known that early life experiences drive gene expression changes and they further influence the maturation of brain and other organs in mammalian individuals, our knowledge about specific epigenetic regulations involved into these processes are limited. Among epigenetic regulations, DNA methylation is known to correlate with gene expression changes that can be used to predict aging and risk level of certain cancer types. However, it is not known if DNA methylation changes might provide a useful 'epigenetic signature' of early-life experiences in an individual child. Therefore, this study addresses two critical questions to understand the nature of DNA methylation changes in early life experiences: (1) does a short period of early postnatal life change methylation patterns in individuals? (2) can methylation changes be used to distinguish individuals with early-life adversity? Consistent with previous studies, these methylation changes cannot distinguish rats with different early life experiences but at different age as distinct groups. We further develop a novel approach and demonstrate for the first time that intra-individual changes in methylation patterns can robustly distinguish individuals with adverse experiences and that they serve as a predictive signature in individuals. Based on this, we expect that this identified DNA signature is commonly shared in rat individuals and should be predictive if it is robust. While it is interesting that rodents would be affected, it would be exciting if this DNA methylation signature of early life maternal also applied to human newborns. In order to allow the future extension of our methods to human infants, we examine methylation by using peripheral cell population from buccal swabs (mixed epithelial and white blood cells) rather than brain cells directly. Given the predictive power of methylation

signature in early life experiences and the accessibility of peripheral cell populations, we will apply in the future this technique to the study of human babies.

Taken together, these findings suggest that early-life experiences set in motion genome-wide changes in methylation patterns of crucial gene-sets, including transcription factors. Early-life adversity associates with altered methylation of gene-sets involved in growth and differentiation as well as response to injury and death. These changes are likely driven by molecular signals, including hormones and nutrients that modulate the complex enzymatic processes that govern DNA methylation status (Borrelli et al. 2008; Doherty and Roth 2018; Moore et al. 2013).

Methods

Animals

Subjects were born to primiparous time-pregnant Sprague-Dawley rat dams (around P75) that were maintained in the quiet animal facility room on a 12 h light/dark cycle with *ad libitum* access to lab chow and water. Parturition was checked daily, and the day of birth was considered postnatal day 0 (P0). Litter size was adjusted 12 per dam on P1, if needed. On P2, pups from several litters were gathered, and 12 pups (6 males and 6 females) were assigned at random to each dam, to obviate the potential confounding effects of genetic variables and of litter size. Each pup was identified by a rapid (<2 minute) foot pad tattooing using animal tattoo ink (Ketchum).

Early-life adversity paradigm

The experimental paradigm involved rearing pups and dams in “impoverished” cages for a week (P2-P9) as described elsewhere (Molet et al. 2014; Ivy et al. 2008; Walker et al. 2017). Briefly, routine rat cages were fitted with a plastic-coated aluminum mesh platform sitting ~2.5 cm above the cage floor (allowing collection of droppings). Bedding was reduced to only cover cage floor sparsely, and one-half of a single paper towel was provided for nesting material, creating a limited bedding and nesting (LBN) cage. Control dams and their litters resided in standard bedded cages, containing 0.33 cubic feet of cob bedding, which was also used for nest building. Control and experimental cages were undisturbed during P2–P9, housed in a quiet room with constant temperature and a strong laminar airflow, preventing ammonia accumulation.

Collection of buccal swab from each pup

The first buccal swab was collected from both cheeks of each pup prior to randomization on P2, using Hydraflock swab (Puritan diagnostics, LLC). After an hour's rest with their mother, a second buccal swab was collected, enabling sufficient DNA from each pup. Pups were then randomized to controls or LBN cages. During P3-P9, behaviors of dams in both control and adversity/LBN cages was observed daily, to ascertain the generation of fragmented unpredictable caring patterns by the adverse environment (Molet et al. 2016; Davis et al. 2017). On P10, buccal swabs were collected as described for P2, then all litters were transferred to normal bedded cages.

Isolation and quantification of DNA for making RRBS libraries from Rat Buccal swab

The Buccal swab was placed into the DNA shields™ (Zymo research) immediately after swabbing. DNA was prepared from the DNA shields solution using the Quick-gDNA™ MiniPrep kit (Zymo Research) following the manufacturer's protocol. The quantity of double stranded DNA was analyzed using Qubit, and RRBS Libraries were prepared from 40 ng of genomic DNA digested with Msp I and then extracted with DNA Clean & Concentrator™-5 kit (Zymo Research). Fragments were ligated to pre-annealed adapters containing 5'-methyl-cytosine instead of cytosine according to Illumina's specified guidelines (www.illumina.com). Adaptor-ligated fragments were then bisulfite-treated using the EZ DNA Methylation-Lightning™ Kit (Zymo Research). Preparative-scale PCR was performed and the resulting products were purified with DNA Clean & Concentrator for sequencing. Amplified RRBS libraries were quantified and qualified by Qubit, Bioanalyzer (Agilent), and Kapa library quant (Kapa systems), and then sequenced on the Illumina NextSeq 500 platform.

RRBS data processing and detection of differentially methylated regions (DMRs)

Adaptor and low quality reads were trimmed and filtered using Trim Galore! 0.4.3 (Krueger F) with parameter '--fastqc --stringency 5 --rrbs --length 30 --non_directional'. Reads were aligned to the rat genome (RGSC 6.0/rn6) by using Bismark 0.16.3 (Krueger and Andrews 2011) with '--non_directional' mode. CpG sites were called by "bismark_methylation_extractor" function from Bismark.

Single CpG sites with more than ten reads coverage were kept for DMR calling. Differential methylation sites (DMSs) were first called using MethyKit (R 3.3.2) (Akalin et al. 2012) with a false discovery rate (FDR) lower than 0.05; DMRs falling within 100 base pairs were then merged.

Calculation of DNA methylation level/percentage and Delta methylation

The methylation percentage/level was calculated as the ratio of the methylated read counts over the sum of both methylated and unmethylated read counts for a single CpG site or across CpGs for a region.

The delta methylation was calculated using the log2 transformation of the ratio of methylation level in the P10 sample and the methylation level in the P2 sample. Increased methylation in P10 is shown as a positive value while decreased methylation in P10 is shown as a negative value.

Principal component analysis (PCA) and K-Means clustering

PCA analysis was performed by using *IncrementalPCA* function from scikit-learn (Pedregosa et al. 2011) using python 2 for both Figure 2 and 3. The value of k was set to 10 for the k-means clustering based on a preliminary hierarchical clustering analysis. A DNA methylation heatmap was generated with heatmap.2 function in R 3.5.0 and a delta methylation heatmap was generated using Java TreeView (Saldanha 2004).

Gene analysis

Genes associated with DMRs were identified using Homer 4.7 (Heinz et al. 2010). For subsequent analyses, genes were kept if (1) CpGs were located within 20kb of TSS in intergenic, promoter-TSS and TTS positions; (2) CpGs were located within gene exons or introns. Gene ontology analysis was performed using Metascape (Tripathi et al. 2015) using the hypergeometric test with corrected P-value lower than 0.05.

Data Access

Reads and processed data from RRBS assays have been submitted to the GEO data repository (http://www.ncbi.nlm.nih.gov/geo/) under accession number XXX.

References

Akalin A, Kormaksson M, Li S, Garrett-Bakelman FE, Figueroa ME, Melnick A, Mason CE. 2012. methylKit: a comprehensive R package for the analysis of genome-wide DNA methylation profiles. *Genome Biol* **13**: R87. https://doi.org/10.1186/gb-2012-13-10-r87.

Bale TL. 2015. Epigenetic and transgenerational reprogramming of brain development. *Nat Rev Neurosci* **16**: 332. http://dx.doi.org/10.1038/nrn3818.

Bale TL, Baram TZ, Brown AS, Goldstein JM, Insel TR, McCarthy MM, Nemeroff CB, Reyes TM, Simerly RB, Susser ES, et al. 2010. Early Life Programming and Neurodevelopmental Disorders. *Biol Psychiatry* **68**: 314–319. http://www.sciencedirect.com/science/article/pii/S0006322310005275.

Bedrosian TA, Quayle C, Novaresi N, Gage FH. 2018. Early life experience drives structural

variation of neural genomes in mice. *Science (80-)* **359**: 1395 LP-1399. http://science.sciencemag.org/content/359/6382/1395.abstract.

Bohacek J, Mansuy IM. 2015. Molecular insights into transgenerational non-genetic inheritance of acquired behaviours. *Nat Rev Genet* **16**: 641. http://dx.doi.org/10.1038/nrg3964.

Bolton JL, Molet J, Regev L, Chen Y, Rismanchi N, Haddad E, Yang DZ, Obenaus A, Baram TZ. 2018. Anhedonia Following Early-Life Adversity Involves Aberrant Interaction of Reward and Anxiety Circuits and Is Reversed by Partial Silencing of Amygdala Corticotropin-Releasing Hormone Gene. *Biol Psychiatry* **83**: 137–147. https://www.sciencedirect.com/science/article/pii/S000632231731942X?via%3Dihub (Accessed April 30, 2018).

Borrelli E, Nestler EJ, Allis CD, Sassone-Corsi P. 2008. Decoding the Epigenetic Language of Neuronal Plasticity. *Neuron* **60**: 961–974. http://dx.doi.org/10.1016/j.neuron.2008.10.012.

Braun P, Hafner M, Nagahama Y, Hing B, McKane M, Grossbach A, Howard M, Kawasaki H, Potash J, Shinozaki G. 2017. Genome-Wide Dna Methylation Comparison Between Live Human Brain and Peripheral Tissues Within Individuals. *Eur Neuropsychopharmacol* **27**: S506. http://www.sciencedirect.com/science/article/pii/S0924977X16308082.

Chen Y, Baram TZ. 2016. Toward Understanding How Early-Life Stress Reprograms Cognitive and Emotional Brain Networks. *Neuropsychopharmacology* **41**: 197–206. http://www.ncbi.nlm.nih.gov/pmc/articles/PMC4677123/.

Consortium TN and PAS of the PG. 2015. Psychiatric genome-wide association study analyses implicate neuronal, immune and histone pathways. *Nat Neurosci* **18**: 199. http://dx.doi.org/10.1038/nn.3922.

Davis EP, Stout SA, Molet J, Vegetabile B, Glynn LM, Sandman CA, Heins K, Stern H, Baram TZ. 2017. Exposure to unpredictable maternal sensory signals influences cognitive development across species. *Proc Natl Acad Sci* **114**: 10390 LP-10395. http://www.pnas.org/content/114/39/10390.abstract.

Davies MN, Volta M, Pidsley R, Lunnon K, Dixit A, Lovestone S, Coarfa C, Harris RA, Milosavljevic A, Troakes C, et al. 2012. Functional annotation of the human brain methylome identifies tissue-specific epigenetic variation across brain and blood. *Genome Biol* **13**: R43. https://doi.org/10.1186/gb-2012-13-6-r43.

Dias BG, Ressler KJ. 2013. Parental olfactory experience influences behavior and neural structure in subsequent generations. *Nat Neurosci* **17**: 89. http://dx.doi.org/10.1038/nn.3594.

Doherty TS, Roth TL. 2018. Epigenetic Landscapes of the Adversity-Exposed Brain. In *Epigenetics and Psychiatric Disease* (ed. D.R.B.T.-P. in M.B. and T.S. Grayson), Vol. 157 of, pp. 1–19, Academic Press http://www.sciencedirect.com/science/article/pii/S187711731730203X.

Eipel M, Mayer F, Arent T, Ferreira MRP, Birkhofer C, Gerstenmaier U, Costa IG, Ritz-Timme S, Wagner W. 2016. Epigenetic age predictions based on buccal swabs are more precise in combination with cell type-specific DNA methylation signatures. *Aging (Albany NY)* **8**: 1034–1044. http://www.ncbi.nlm.nih.gov/pmc/articles/PMC4931852/.

Heinz S, Benner C, Spann N, Bertolino E, Lin YC, Laslo P, Cheng JX, Murre C, Singh H, Glass CK. 2010. Simple Combinations of Lineage-Determining Transcription Factors Prime cis-Regulatory Elements Required for Macrophage and B Cell Identities. *Mol Cell* **38**: 576–589. http://www.sciencedirect.com/science/article/pii/S1097276510003667.

Horvath S, Raj K. 2018. DNA methylation-based biomarkers and the epigenetic clock theory of ageing. *Nat Rev Genet* **19**: 371–384. https://doi.org/10.1038/s41576-018-0004-3.

Ivy AS, Brunson KL, Sandman C, Baram TZ. 2008. Dysfunctional nurturing behavior in rat dams with limited access to nesting material: A clinically relevant model for early-life stress. *Neuroscience* **154**: 1132–1142. http://www.sciencedirect.com/science/article/pii/S0306452208005630.

Ivy AS, Rex CS, Chen Y, Dubé C, Maras PM, Grigoriadis DE, Gall CM, Lynch G, Baram TZ. 2010. Hippocampal Dysfunction and Cognitive Impairments Provoked by Chronic Early-Life Stress Involve Excessive Activation of CRH Receptors. *J Neurosci* **30**: 13005–13015. http://www.jneurosci.org/content/jneuro/30/39/13005.full.pdf.

Klengel T, Binder EB. 2015. Epigenetics of Stress-Related Psychiatric Disorders and Gene × Environment Interactions. *Neuron* **86**: 1343–1357. http://www.sciencedirect.com/science/article/pii/S0896627315004754.

Krueger F. Trim Galore! http://www.bioinformatics.babraham.ac.uk/projects/trim_galore/.

Krueger F, Andrews SR. 2011. Bismark: a flexible aligner and methylation caller for Bisulfite-Seq applications. *Bioinformatics* **27**: 1571–1572. http://dx.doi.org/10.1093/bioinformatics/btr167.

Lister R, Mukamel EA, Nery JR, Urich M, Puddifoot CA, Johnson ND, Lucero J, Huang Y, Dwork AJ, Schultz MD, et al. 2013. Global Epigenomic Reconfiguration During Mammalian Brain Development. *Science (80-)* **341**. http://science.sciencemag.org/content/341/6146/1237905.abstract.

Lowe R, Gemma C, Beyan H, Hawa MI, Bazeos A, Leslie RD, Montpetit A, Rakyan VK, Ramagopalan S V. 2013. Buccals are likely to be a more informative surrogate tissue than blood for epigenome-wide association studies. *Epigenetics* **8**: 445–454. https://doi.org/10.4161/epi.24362.

Meissner A, Gnirke A, Bell GW, Ramsahoye B, Lander ES, Jaenisch R. 2005. Reduced representation bisulfite sequencing for comparative high-resolution DNA methylation analysis. *Nucleic Acids Res* **33**: 5868–5877. http://www.ncbi.nlm.nih.gov/pmc/articles/PMC1258174/.

Molet J, Heins K, Zhuo X, Mei YT, Regev L, Baram TZ, Stern H. 2016. Fragmentation and high entropy of neonatal experience predict adolescent emotional outcome. *Transl Psychiatry* **6**: e702. http://dx.doi.org/10.1038/tp.2015.200.

Molet J, Maras PM, Avishai-Eliner S, Baram TZ. 2014. Naturalistic rodent models of chronic early-life stress. *Dev Psychobiol* **56**: 1675–1688. https://onlinelibrary.wiley.com/doi/abs/10.1002/dev.21230.

Moore LD, Le T, Fan G. 2013. DNA Methylation and Its Basic Function. *Neuropsychopharmacology* **38**: 23–38. http://www.ncbi.nlm.nih.gov/pmc/articles/PMC3521964/.

Nelson CA, Zeanah CH, Fox NA, Marshall PJ, Smyke AT, Guthrie D. 2007. Cognitive Recovery in Socially Deprived Young Children: The Bucharest Early Intervention Project. *Science (80-)* **318**: 1937 LP-1940. http://science.sciencemag.org/content/318/5858/1937.abstract.

Nemoda Z, Massart R, Suderman M, Hallett M, Li T, Coote M, Cody N, Sun ZS, Soares CN, Turecki G, et al. 2015. Maternal depression is associated with DNA methylation changes in cord blood T lymphocytes and adult hippocampi. *Transl Psychiatry* **5**: e545. http://dx.doi.org/10.1038/tp.2015.32.

Nestler EJ, Peña CJ, Kundakovic M, Mitchell A, Akbarian S. 2015. Epigenetic Basis of Mental Illness. *Neurosci* **22**: 447–463. https://doi.org/10.1177/1073858415608147.

Pedregosa F, Varoquaux G, Gramfort A, Michel V, Thirion B, Grisel O, Blondel M, Prettenhofer P, Weiss R, Dubourg V, et al. 2011. Scikit-learn: Machine Learning in Python. *J Mach Learn Res* **12**: 2825–2830. http://dl.acm.org/citation.cfm?id=1953048.2078195.

Peter CJ, Fischer LK, Kundakovic M, Garg P, Jakovcevski M, Dincer A, Amaral AC, Ginns EI, Galdzicka M, Bryce CP, et al. 2016. DNA Methylation Signatures of Early Childhood Malnutrition Associated With Impairments in Attention and Cognition. *Biol Psychiatry* **80**: 765–774. http://dx.doi.org/10.1016/j.biopsych.2016.03.2100.

Reizel Y, Sabag O, Skversky Y, Spiro A, Steinberg B, Bernstein D, Wang A, Kieckhaefer J, Li C, Pikarsky E, et al. 2018. Postnatal DNA demethylation and its role in tissue maturation. *Nat Commun* **9**: 2040. https://doi.org/10.1038/s41467-018-04456-6.

Said M, Cappiello C, Devaney JM, Podini D, Beres AL, Vukmanovic S, Rais-Bahrami K, Luban NC, Sandler AD, Tatari-Calderone Z. 2014. Genomics In Premature Infants: A Non-Invasive Strategy To Obtain High-Quality DNA. *Sci Rep* **4**: 4286. http://www.ncbi.nlm.nih.gov/pmc/articles/PMC3944721/.

Saldanha AJ. 2004. Java Treeview—extensible visualization of microarray data. *Bioinformatics* **20**: 3246–3248. http://dx.doi.org/10.1093/bioinformatics/bth349.

Singh-Taylor A, Molet J, Jiang S, Korosi A, Bolton JL, Noam Y, Simeone K, Cope J, Chen Y, Mortazavi A, et al. 2017. NRSF-dependent epigenetic mechanisms contribute to programming of stress-sensitive neurons by neonatal experience, promoting resilience. *Mol Psychiatry* **23**: 648. http://dx.doi.org/10.1038/mp.2016.240.

Smith AK, Kilaru V, Klengel T, Mercer KB, Bradley B, Conneely KN, Ressler KJ, Binder EB. 2015. DNA extracted from saliva for methylation studies of psychiatric traits: Evidence tissue specificity and relatedness to brain. *Am J Med Genet Part B Neuropsychiatr Genet* **168**: 36–44. https://onlinelibrary.wiley.com/doi/abs/10.1002/ajmg.b.32278.

Szyf M. 2015. Nongenetic inheritance and transgenerational epigenetics. *Trends Mol Med* **21**: 134–144. http://www.sciencedirect.com/science/article/pii/S1471491414002184.

Tripathi S, Pohl MO, Zhou Y, Rodriguez-Frandsen A, Wang G, Stein DA, Moulton HM, DeJesus P, Che J, Mulder LCF, et al. 2015. Meta- and Orthogonal Integration of Influenza "OMICs" Data Defines a Role for UBR4 in Virus Budding. *Cell Host Microbe* **18**: 723–735. http://www.sciencedirect.com/science/article/pii/S1931312815004564.

Walker C-D, Bath KG, Joels M, Korosi A, Larauche M, Lucassen PJ, Morris MJ, Raineki C, Roth TL, Sullivan RM, et al. 2017. Chronic early life stress induced by limited bedding and nesting (LBN) material in rodents: critical considerations of methodology, outcomes and translational potential. *Stress* **20**: 421–448. https://doi.org/10.1080/10253890.2017.1343296.

Weaver ICG, Cervoni N, Champagne FA, D'Alessio AC, Sharma S, Seckl JR, Dymov S, Szyf M, Meaney MJ. 2004. Epigenetic programming by maternal behavior. *Nat Neurosci* **7**: 847. http://dx.doi.org/10.1038/nn1276.

Figures

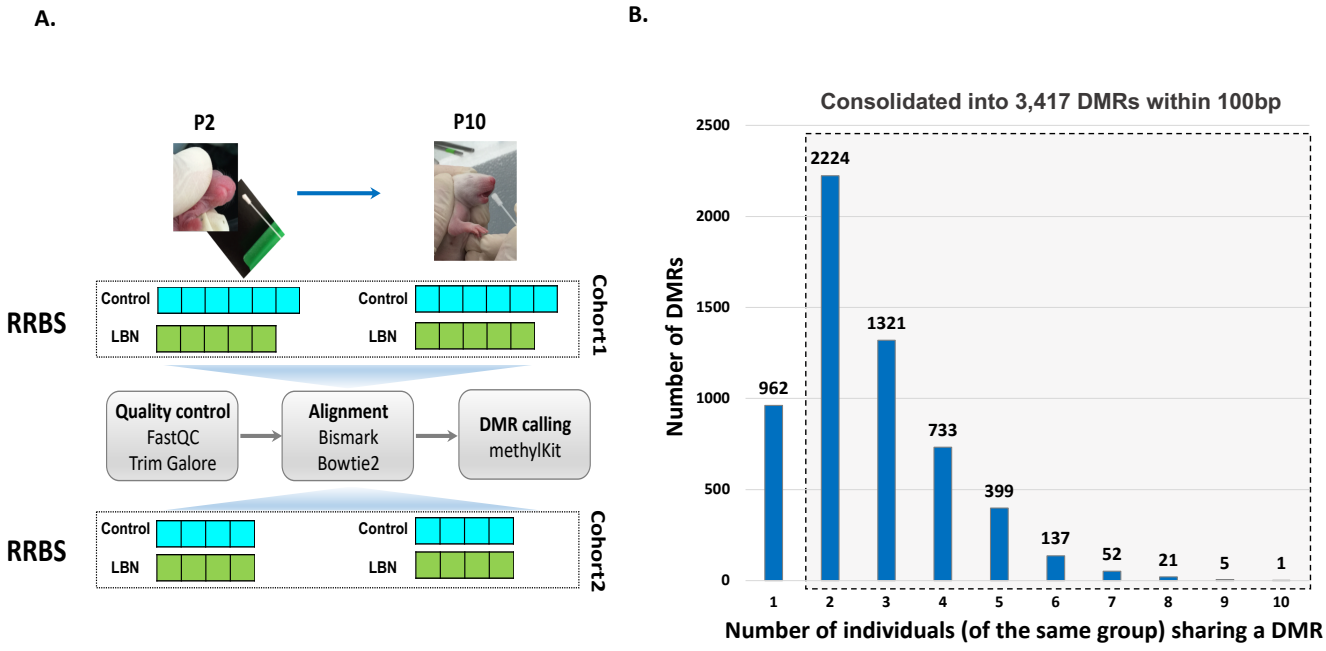

Figure 1. (A) Experimental design and analysis pipeline. (B) Histogram of the number of significant differentially methylated regions (DMRs) based on the number of individuals sharing the same experience. RRBS = reduced representation bisulfite sequencing; LBN-limited nesting and bedding cages, a paradigm of adversity. P2,P10 = postnatal days 2,10.

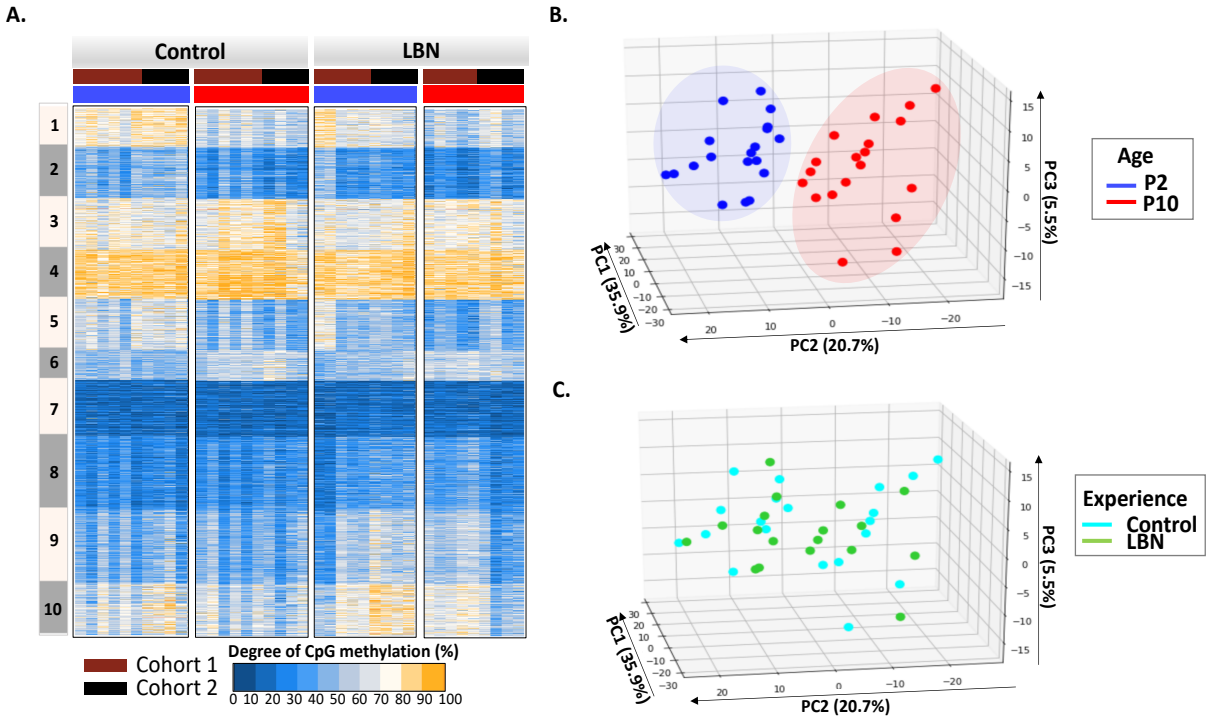

Figure 2. (A) Heatmap of CpG methylation percentage on 3,417 DMRs across individuals. The profile is presented into 10 clusters that are clustered using K-means clustering. Blue, low methylation percentage; orange, high methylation percentage. (B) Principal component analysis (PCA) of individuals on 3,417 DMRs. Individuals are labeled by age, P2, blue; P10, red. (C) Principal component analysis (PCA) of individuals on 3,417 DMRs. Individuals are labeled by experience, Control, cyan; LBN, green.

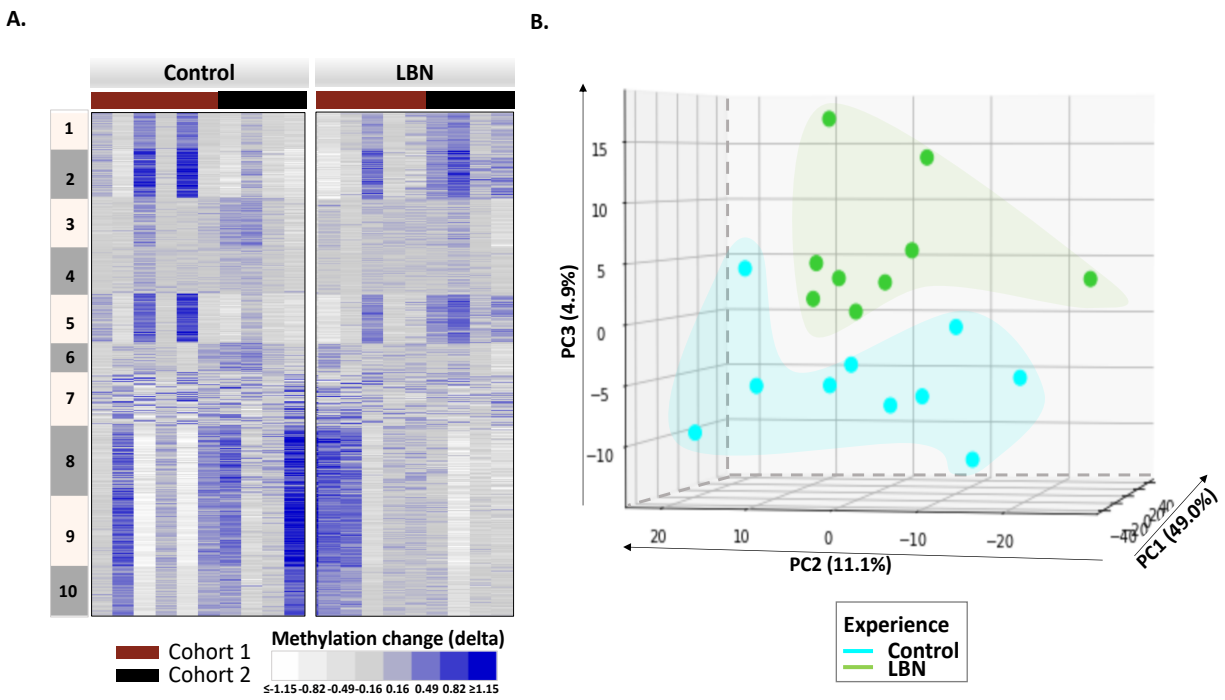

Figure 3. (A) Heatmap of delta methylation between P10 and P2 (log2(P10/P2)) of 3,417 DMRs. DMRs are in the same order as in Figure2A. (B) Principal component analysis (PCA) of the DMRs of individuals labeled by experience, Control, cyan; LBN, green.

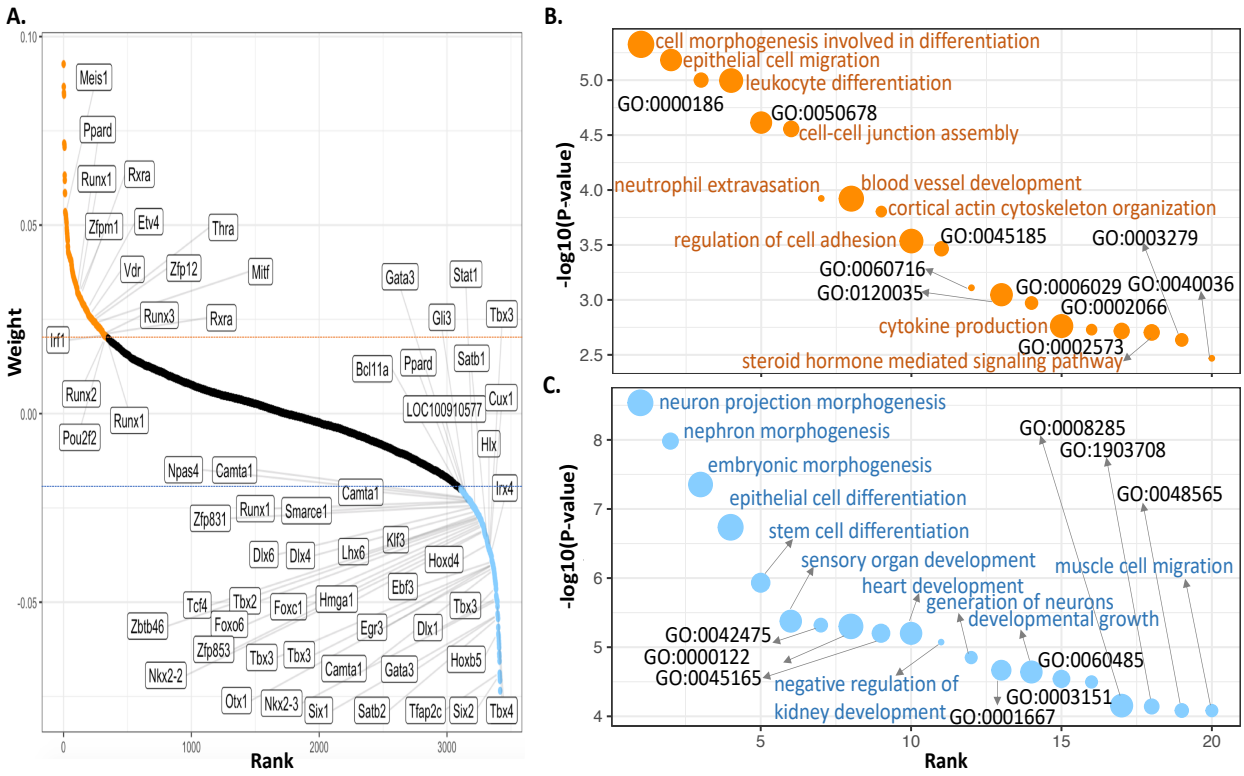

Figure 4. Analysis of PC3 weights (A) Most significant positive (orange) and negative (blue) weights are enriched in transcription factors. (B) GO terms of genes associated with 346 most positively weighted DMRs (orange) in 4A. (C) GO terms of genes associated with 311 most negatively weighted DMRs (blue) in 4A.

Supplementary figures

A.

Cohort1

P2	Mapped reads (million)	Efficiency	P10	Mapped reads (million)	Efficiency
P2C3	13	43.30%	P10C3	23	46.00%
P2C4	9	36.1%	P10C4	19	55.1%
P2C6	12	51.30%	P10C6	17	44.40%
P2C7	22	59.50%	P10C7	26	52.00%
P2C9	18	41.10%	P10C9	26	53.70%
P2C12	20	49.20%	P10C12	24	52.20%
P2LBN2	15	39.90%	P10LBN2	11	45.90%
P2LBN3	18	43.20%	P10LBN3	30	58.90%
P2LBN4	23	48.80%	P10LBN4	28	51.00%
P2LBN9	12	46.40%	P10LBN9	24	50.40%
P2LBN12	15	45.40%	P10LBN12	26	56.40%

Individual	Detected CpGs in both P2 and P10	Significant DMRs
C3	418860	870
C4	358726	4664
C6	404260	4384
C7	521418	1959
C9	514738	2679
C12	496953	2318
LBN2	415216	5540
LBN3	482076	6345
LBN4	539139	629
LBN9	418466	1851
LBN12	443196	1963

B.

Cohort2

P2	Mapped reads (million)	Efficiency	P10	Mapped reads (million)	Efficiency
P2C1	21	46.0%	P10C1	22	42.5%
P2C5	20	47.4%	P10C5	20	45.6%
P2C8	17	60.4%	P10C8	22	49.2%
P2C11	19	55.7%	P10C11	27	58.1%
P2LBN2	28	57.8%	P10LBN2	30	61.9%
P2LBN4	21	49.2%	P10LBN4	20	42.0%
P2LBN9	21	45.8%	P10LBN9	22	54.2%
P2LBN11	23	47.2%	P10LBN11	20	50.8%

Individual	Detected CpGs in both P2 and P10	Significant DMRs
C1	510525	3073
C5	505100	1879
C8	508787	1278
C11	525733	7040
LBN2	584480	1064
LBN4	498882	2566
LBN9	521111	1190
LBN11	504507	2745

Figure S1. RRBS QC matrix for cohort1 **(A)** and cohort2 **(B),** including the number of uniquely mapped reads, mapping efficiency and significant DMRs calling for each individual.

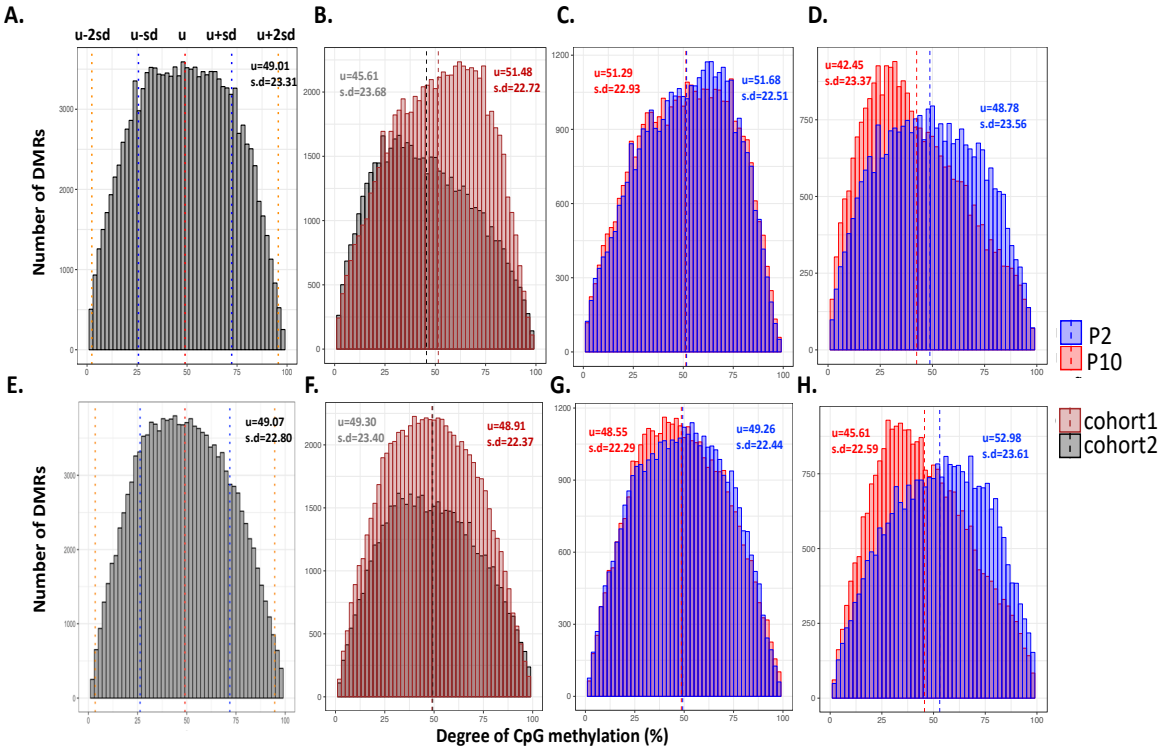

Figure S2. (A) Histogram of DNA methylation level on 3,417 DMRs across 19 individuals from two cohorts before batch correction by cohorts. For each DMR, each individual has one methylation level for P2 and one for P10. 11 individuals are in cohort1 and 8 individuals are in cohort2.
(B) Histogram of DNA methylation level on 3,417 DMRs for two cohorts separately (before correction by cohorts).
(C) Histogram of DNA methylation level on 3,417 DMRs on cohort1 for P2 and P10 separately (before correction by cohorts).
(D) Histogram of DNA methylation level on 3,417 DMRs on cohort2 for P2 and P10 separately (before correction by cohorts).
(E) Histogram of DNA methylation level on 3,417 DMRs across 19 individuals from two cohorts after correction by cohorts. For each DMR, each individual has one methylation level for P2 and one for P10. 11 individuals are in cohort1 and 8 individuals are in cohort2.
(F) Histogram of DNA methylation level on 3,417 DMRs for two cohorts separately (after correction by cohorts).
(G) Histogram of DNA methylation level on 3,417 DMRs on cohort1 for P2 and P10 separately (after correction by cohorts).
(H) Histogram of DNA methylation level on 3,417 DMRs on cohort2 for P2 and P10 separately (after correction by cohorts).
u represents mean value; s.d represent standard deviation.

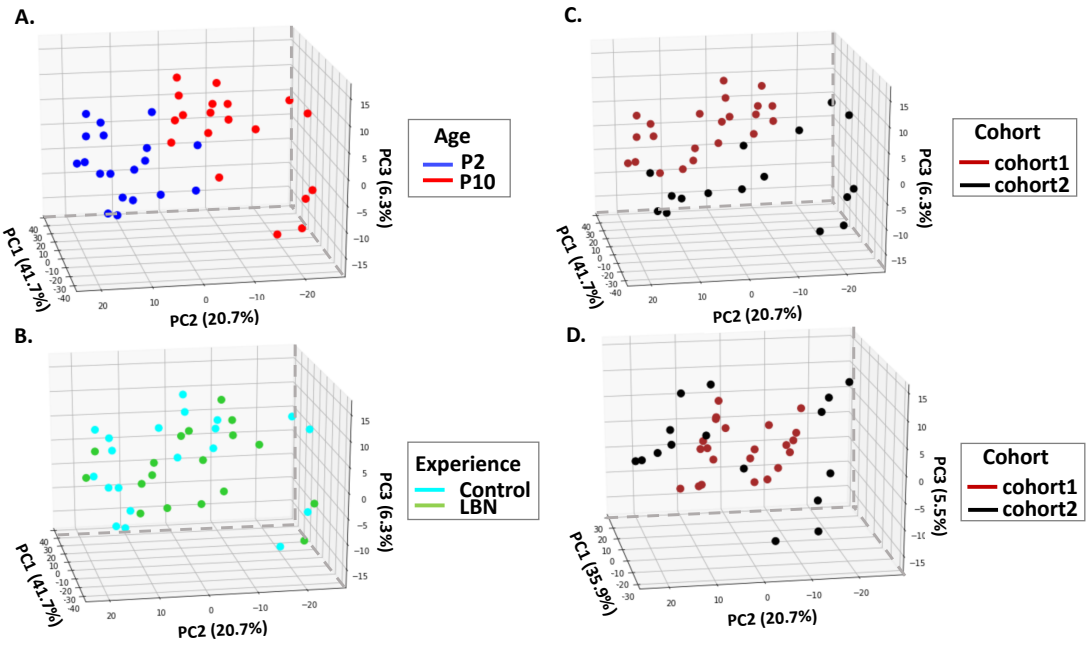

Figure S3. PCA analysis on 3,417 DMRs before batch correction by cohort and labeled by **(A)** age, **(B)** experience and **(C)** cohort. **(D)** PCA on 3,417 DMRs after batch correction by cohort. Figure S3D is the same PCA as shown in Figure 2B and C now labeled by cohort.

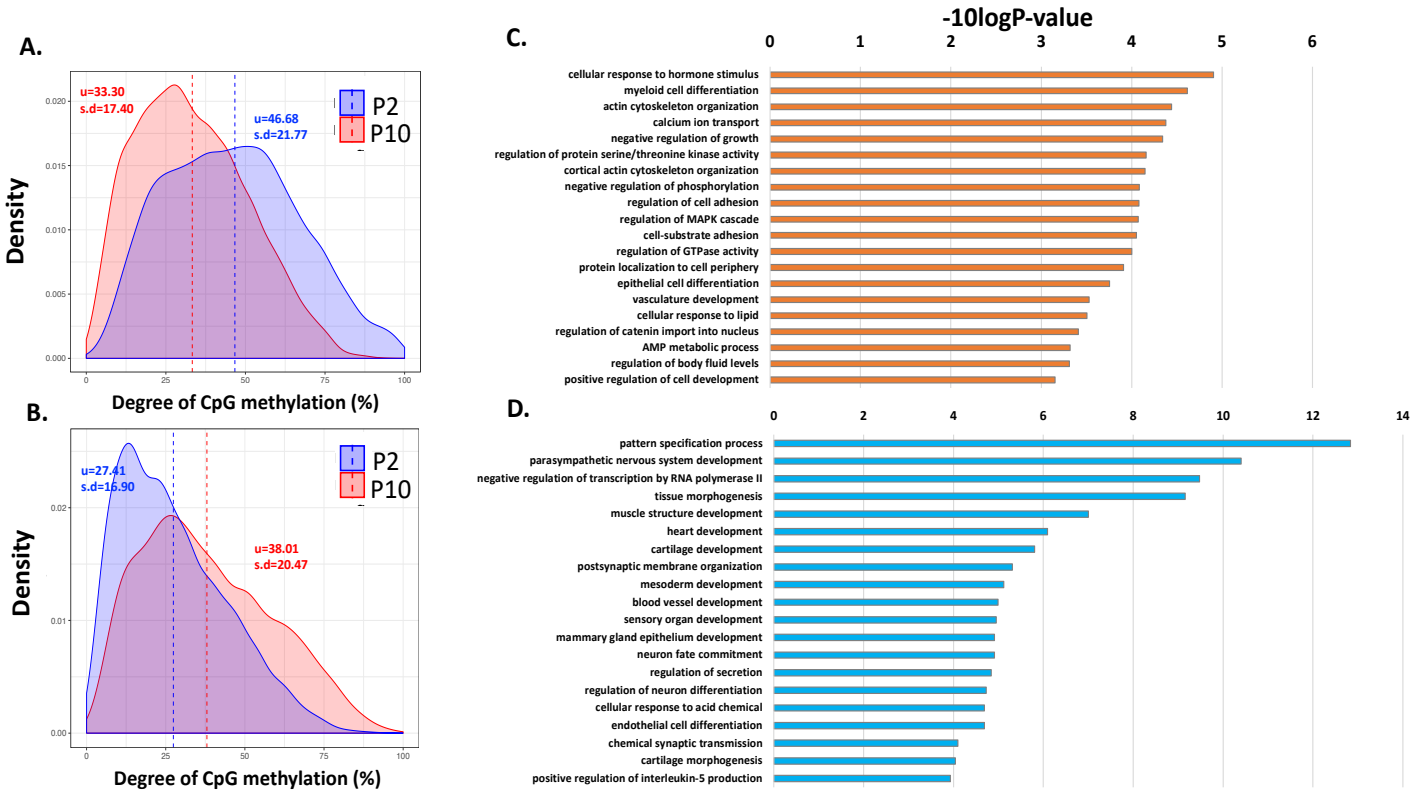

Figure S4. (A) DNA methylation level of top-positive DMRs (from PC2 in Figure2B) and density distributions are plotted by age separately.
(B) DNA methylation level of bottom-negative DMRs (from PC2 in Figure2B) and density distributions are plotted by age separately.
(C) Gene ontology terms enriched in genes associated with top-positive DMRs.
(D) Gene ontology terms enriched in genes associated with bottom-negative DMRs.

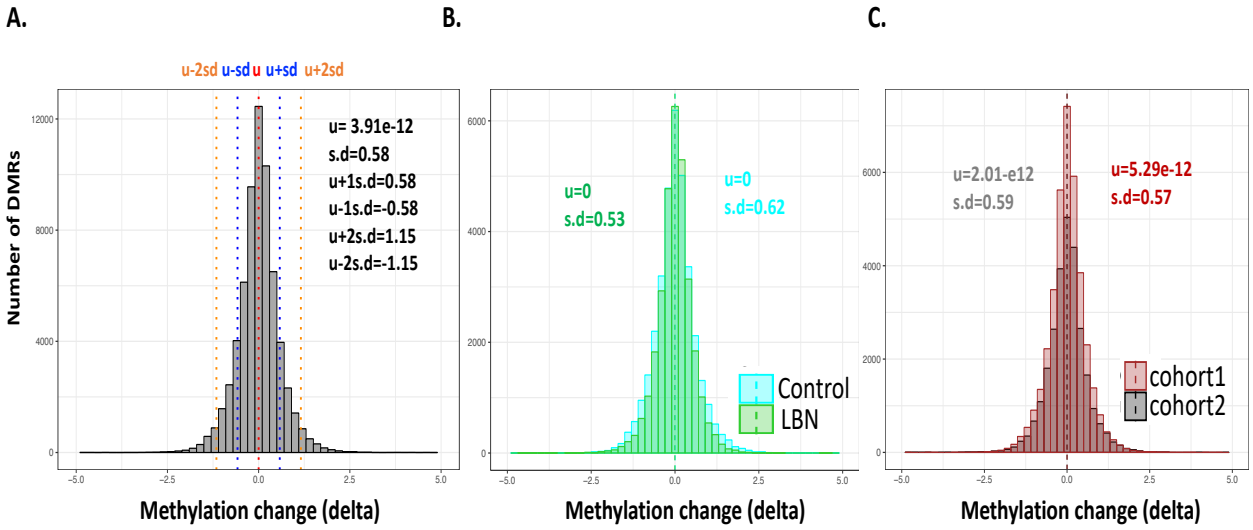

Figure S5. (A) Histogram of delta DNA methylation on 3,417 DMRs across 19 individuals from two cohorts.
(B) Histogram of delta DNA methylation on 3,417 DMRs for control and LBN separately.
(C) Histogram of delta DNA methylation on 3,417 DMRs for two cohorts separately.
u represents mean value; s.d represent standard deviation.

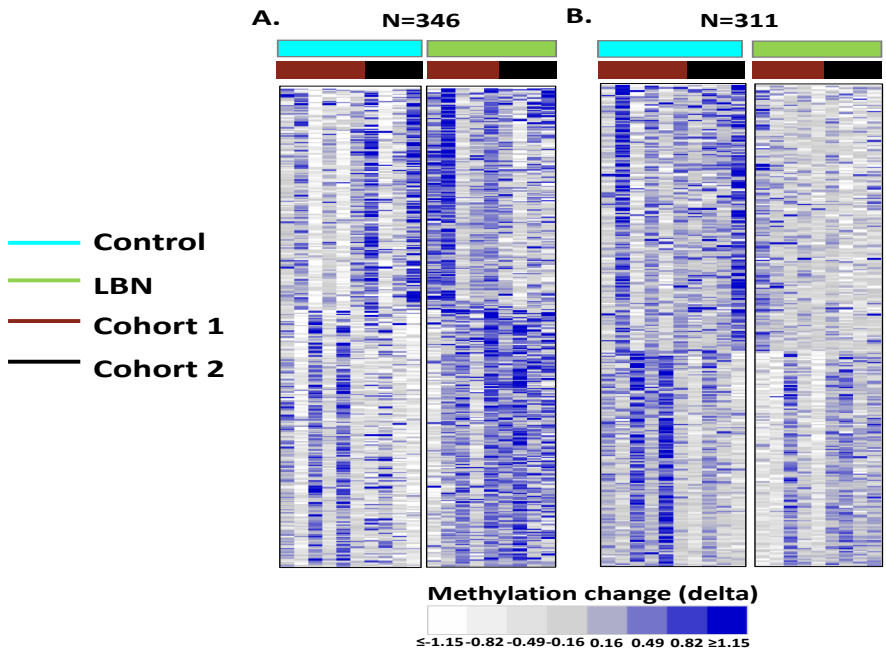

Figure S6. Heatmap of delta methylation changing profiles between P10 and P2 on **657** DMRs (top weights were collected from PC3 in Figure 3B, which can separate control and LBN). **(A)** 346 "top-positive" weights predict LBN, showing increased methylation in P10 LBN while **(B)** 311 "bottom-negative" weights predict control, showing increased methylation in P10 Control.

A.

Categories	Gene symbol	Number of genes
Transcription factor	Sim2, Meis1,Ppard, Runx1, Zfpm1, Rxra, Etv4, Thra, Zfp12, Mitf, Runx3, Irf1, Runx2,Pou2f2, Vdr	15
Growth and Growth factos	Tgfbr3,Sipa1,Map3k8,Rai1,Net1,Mark2,Prkd2,Paqr6,Ltbp1,Heg1,Rxra,Parp16,Cdk6,Map3k5,Map3k13,Srcin1,Fitm1,Akap2,Pik3cd,Prkar1b,Ros1, Kidins220,Mark3,Egfl7,Mast3,Stk36	26
Inflammation/ Injury/ Death	Pdcd6ip,Tnfrsf1b,Card10,Lsp1,Cd83,Traf3,Ppard,Gadd45b,Ercc1,Tbxas1,Cxcr1,Sipa1l3,Bmf,Klk9,Tnfrsf19,Dnajb12,Traf1,Irf2bpl, Glipr2, Azi2,Rxra,Nfkbil1,Irf1,Hspbap1,C1qtnf5	25
Solute and other transport	Sys1,Gpr39,Slc44a3,Ffar4,Slc26a9,RGD1307315,Apba2,Cacng4,Kcnk5,Slc7a1,Ros1,Mcart1,Cnnm2, Slc25a33,Ric1	15
Neuron projection/guidance/ cell morphogenesis, differentiation	Mark2,Cxcr4,Nrp2,Sema5b,Ptpro,Fam129b,Sema4a,Efnb2,Sec24b,Srcin1,Llgl1,Srcin1,Pik3cd,Sema3g,Kidins220,Fbxw8,Clic5,Ank3	18
Steroid hormone mediated signaling pathway	Paqr6,Ffar4,Bcan,Ppard,Rxra,Vdr,Abhd2,Thra,Cdh13	9

B.

Categories	Gene symbol	Number of genes
Transcription factor	Nkx2-3,Six2,Tfap2c,Tbx4,Hoxb5,Satb2,Gata3,Six1, Dlx1,Tbx3,Otx1,Egr3,Ebf3,Irx4,Cux1,Hlx,Hoxd4,Satb1,Hmga1,Nkx2-2, Zfp853,Foxc1,Foxo6,Tbx2,Zbtb46,Tcf4,Lhx6,Klf3,Dlx4,Stat1,Dlx6,Zfp831,Smarce1,Runx1,Camta1,Npas4,Gli3, LOC100910577,Ppard,Bcl11a	40
Kinase	Akap6,Dapk1,Limk2,Kalrn,Sgk1,Kit,Mos,Taok3,Prkca,Map2k6,Ak7	11
Inflammation/ Injury/ Death	Tnfaip2,Dapk1,Cd37,Bmf,Slc44a2,Hsp90b1,Dedd2,Il20rb,Ptpn13,Slc25a37,Ppard	11
Solute and other transport	Osbpl1a,Atp8b1,Kif5c,Slc44a2,Ddx20,Cct8,Abcc12,Gltp,Slc3a1,Slc4a4,Slc43a3,Abcg4,Slc25a37,Slc35g1,Kcnn4,Slc38a1, Kcng1,Atp8a2,Kif26b,Tspo,Slc36a1	21
cytoskeleton / cell morphogenesis /projection/synapse	Sema4d,Gdnf,Six2,Strip1,Fzd2,Atp8b1,Atp8b1,Akap6,Crmp1,Tbx3,Myl2,Rims2,Dnmbp,Egr3,Tbx3,Fzd7,Atxn2,Nrp1,Syngap1,Fgf4,Tbx3,Hlx,Kalrn,Syt7,Ankrd55,Sema6c,Agap3,Ppp1r16b,Dedd2,Hmga1,Arhgef4,Sema3b,Itga10,Sgk1,Zbtb46,Bmp7,Kit,Mfap2,Rheb,B3gnt2,Smg6,Mos,Slit3,Dock5,Rab3gap2,LOC102552318,Nrxn2,Kif26b,Arrdc3,Icam1,Tspo, Celsr1,Nkx2-2	53

Supplemental Table 1. Annotation and classification of genes associated with “positive” and “negative” weights (0.02 cutoff) of PC3 in Figure 4A. (A) genes associated with “positive” weights (B) genes associated with “negative” weights.